AGU PUBLICATIONS

Global Biogeochemical Cycles

RESEARCH ARTICLE
10.1002/2015GB005350

Key Points:
- $\delta^{15}N$ and $\delta^{18}O$ of $NO_3^- + NO_2^-$ and NO_3^--only suggest expression of NO_3^--NO_2^- equilibrium isotope effect, likely due to enzyme reversibility
- Interconversion of NO_3^- and NO_2^- is correlated with seasonal mixed layer deepening and suggests a role for entrained NO_2^- oxidizers
- Interconversion may occur where NO_2^- oxidizers are transported into regions that inhibit NO_2^- oxidation, including oxygen-deficient zones

Supporting Information:
- Supporting Information S1

Correspondence to:
P. C. Kemeny,
pkemeny@princeton.edu

Citation:
Kemeny, P. C., M. A. Weigand, R. Zhang, B. R. Carter, K. L. Karsh, S. E. Fawcett, and D. M. Sigman (2016), Enzyme-level interconversion of nitrate and nitrite in the fall mixed layer of the Antarctic Ocean, *Global Biogeochem. Cycles*, *30*, 1069–1085, doi:10.1002/2015GB005350.

Received 8 DEC 2015
Accepted 13 JUN 2016
Accepted article online 20 JUN 2016
Published online 13 JUL 2016

Enzyme-level interconversion of nitrate and nitrite in the fall mixed layer of the Antarctic Ocean

P. C. Kemeny[1,2], M. A. Weigand[1], R. Zhang[3], B. R. Carter[4,5], K. L. Karsh[6], S. E. Fawcett[7], and D. M. Sigman[1]

[1]Department of Geosciences, Princeton University, Princeton, New Jersey, USA, [2]Division of Geological and Planetary Sciences, California Institute of Technology, Pasadena, California, USA, [3]College of Ocean and Earth Sciences, Xiamen University, Xiamen, China, [4]Joint Institute for the Study of the Atmosphere and Ocean, University of Washington, Seattle, Washington, USA, [5]NOAA Pacific Marine Environmental Laboratory, Seattle, Washington, USA, [6]Antarctic Climate & Ecosystems Cooperative Research Centre, University of Tasmania, Hobart, Tasmania, Australia, [7]Department of Oceanography, University of Cape Town, Rondebosch, South Africa

Abstract In the Southern Ocean, the nitrogen (N) isotopes of organic matter and the N and oxygen (O) isotopes of nitrate (NO_3^-) have been used to investigate NO_3^- assimilation and N cycling in the summertime period of phytoplankton growth, both today and in the past. However, recent studies indicate the significance of processes in other seasons for producing the annual cycle of N isotope changes. This study explores the impact of fall conditions on the $^{15}N/^{14}N$ ($\delta^{15}N$) and $^{18}O/^{16}O$ ($\delta^{18}O$) of NO_3^- and nitrite (NO_2^-) in the Pacific Antarctic Zone using depth profiles from late summer/fall of 2014. In the mixed layer, the $\delta^{15}N$ and $\delta^{18}O$ of $NO_3^- + NO_2^-$ increase roughly equally, as expected for NO_3^- assimilation; however, the $\delta^{15}N$ of NO_3^--only (measured after NO_2^- removal) increases more than does NO_3^--only $\delta^{18}O$. Differencing indicates that NO_2^- has an extremely low $\delta^{15}N$, often $< -70‰$ versus air. These observations are consistent with the expression of an equilibrium N isotope effect between NO_3^- and NO_2^-, likely due to enzymatic NO_3^--NO_2^- interconversion. Specifically, we propose reversibility of the nitrite oxidoreductase (NXR) enzyme of nitrite oxidizers that, having been entrained from the subsurface during late summer mixed layer deepening, are inhibited by light. Our interpretation suggests a role for NO_3^--NO_2^- interconversion where nitrifiers are transported into environments that discourage NO_2^- oxidation. This may apply to surface regions with upwelling, such as the summertime Antarctic. It may also apply to oxygen-deficient zones, where NXR-catalyzed interconversion may explain previously reported evidence of NO_2^- oxidation.

1. Introduction

Production and export of organic carbon from the high-latitude surface ocean lowers the atmospheric concentration of carbon dioxide (CO_2) directly through the removal of dissolved inorganic carbon to the deep ocean and indirectly by driving an increase in whole-ocean alkalinity [*Sigman and Boyle*, 2000]. In the modern Southern Ocean, nutrient consumption in surface waters is incomplete due to limitation of phytoplankton by iron and light [*Martin*, 1990; *Sunda and Huntsman*, 1997]. The upper ocean surrounding Antarctica is thus enriched in nitrogen (N) and phosphorus (P), the production and export of organic carbon is much less than potential export [*Reuer et al*., 2007], and much of the upwelled CO_2 degasses to the atmosphere [*Sigman et al*., 2010]. Increasing nutrient consumption in the Southern Ocean could stem this CO_2 leakage and has been proposed as an explanation for the lower atmospheric CO_2 concentrations of past ice ages [*Knox and McElroy*, 1984; *Sarmiento and Toggweiler*, 1984; *Siegenthaler and Wenk*, 1984].

In the Antarctic Zone (AZ), the southernmost region of the Southern Ocean, nutrients are supplied to the surface ocean through seasonal mixing and wind-driven upwelling. In winter, the Antarctic surface cools and increases in salinity due to sea ice formation, deepening the mixed layer and importing nutrients from the deep ocean into surface waters. Furthermore, NO_3^--rich deep water upwells into the surface ocean due to Ekman divergence induced by circumpolar westerly winds. During summer, surface warming melts the ice and shoals the mixed layer, stratifying the water column. No longer light-limited, phytoplankton in the summertime mixed layer draw down NO_3^- and other nutrients. The water below the summertime mixed layer, which was the base of the winter mixed layer, retains the low temperatures of the Antarctic winter and is called the temperature minimum (T_{min}) layer. The T_{min} layer is thought to be a summertime record of winter

conditions as well as a reflection of the initial state from which the surface ocean evolves throughout the summer [*Altabet and Francois*, 2001].

The $^{15}N/^{14}N$ and $^{18}O/^{16}O$ ratios of seawater NO_3^- can be used to study nutrient consumption in the Southern Ocean. Phytoplankton consuming surface NO_3^- preferentially assimilate the lighter isotopes of nitrogen and oxygen, ^{14}N and ^{16}O, relative to the heavier isotopes, ^{15}N and ^{18}O [*Wada and Hattori*, 1978; *Pennock et al*., 1996; *Waser et al*., 1998; *Needoba et al*., 2004], such that consumption increases the $\delta^{15}N$ ($([^{15}N/^{14}N]_{sample}/[^{15}N/^{14}N]_{air} - 1) \times 1000$) and $\delta^{18}O$ ($([^{18}O/^{16}O]_{sample}/[^{18}O/^{16}O]_{VSMOW} - 1) \times 1000$) of the NO_3^- remaining in seawater. This isotopic change in the NO_3^- pool is commonly simulated using the Rayleigh model, which describes an approximately linear relationship between the $\delta^{15}N$ of the NO_3^- substrate and the natural logarithm of the fraction of NO_3^- remaining [*Mariotti et al*., 1981]. The slope of the line approximates $^{15}\varepsilon$, the N isotope effect for nitrate assimilation, which is defined as $^{15}\varepsilon = (^{14}k/^{15}k - 1) \times 1000$, where ^{14}k and ^{15}k are the rate coefficients for the assimilation of ^{14}N and ^{15}N-bearing NO_3^-, respectively. Below, we refer to plots of NO_3^- $\delta^{15}N$ or $\delta^{18}O$ against the natural logarithm of NO_3^- as "Rayleigh space." The Rayleigh model assumes a closed substrate pool, which is largely the case for NO_3^- in the AZ during the summer, when NO_3^- supply is weak relative to NO_3^- assimilation. Moreover, because the fractional consumption of NO_3^- in the summertime surface is relatively low, violations of the Rayleigh model assumptions due to Ekman-driven NO_3^- supply or in situ remineralization have minimal effect [*Sigman et al*., 1999].

The Rayleigh model, however, fails to capture seasonal patterns in the $\delta^{15}N$ and $\delta^{18}O$ of NO_3^-, which recent studies of NO_3^- and NO_2^- isotopes from the Southern Ocean have begun to document [*DiFiore et al*., 2010; *Smart et al*., 2015]. In particular, the Rayleigh model fails to explain the chemistry of the temperature minimum layer, due at least in part to wintertime nitrification of the low-$\delta^{15}N$ NH_4^+ resulting from intensive biological N recycling in the late summer mixed layer [*Lourey et al*., 2003; *Smart et al*., 2015].

This study provides additional insights into the seasonal origin of non-Rayleigh NO_3^- isotope dynamics in the Southern Ocean. We report $\delta^{15}N$ and $\delta^{18}O$ for both $NO_3^- + NO_2^-$ and NO_3^--only in samples from eight profiles collected in the Pacific Antarctic Zone during the 2014 U.S. Repeat Hydrography cruise along the P16S line. In the combined $NO_3^- + NO_2^-$ data, we recover the previously observed non-Rayleigh behavior of the T_{min} layer and derive values for the N and O isotope effects of NO_3^- assimilation that are consistent with prior estimates from the region. The coupled N and O isotope measurements of the combined $NO_3^- + NO_2^-$ pool indicate close to equivalent increases in $\delta^{15}N$ and $\delta^{18}O$ into the surface mixed layer, consistent with expectations for NO_3^- assimilation from culture studies [*Granger et al*., 2004, 2008, 2010; *Karsh et al*., 2012, 2014].

However, we find that the $\delta^{15}N$ of NO_3^--only increases more than does the $\delta^{18}O$ of NO_3^--only, which is not expected given known Southern Ocean processes. By differencing the $NO_3^- + NO_2^-$ and NO_3^--only measurements, we calculate very low values for NO_2^- $\delta^{15}N$ in the upper ~90 m. These observations suggest the expression of an equilibrium N isotope effect between NO_3^- and NO_2^- in the late summer surface ocean, which preferentially partitions ^{15}N into NO_3^- and ^{14}N into NO_2^-. This equilibration could result from the bidirectional interconversion of NO_3^- and NO_2^-, likely catalyzed by biochemical reaction reversibility. The NO_2^- oxidoreductase (NXR) enzyme, a bidirectional enzyme in certain nitrifying microorganisms that catalyzes both the oxidation of NO_2^- and the reduction of NO_3^- [*Sundermeyer-Klinger et al*., 1984], has previously been implicated in isotope exchange between NO_2^- and NO_3^- [*Friedman et al*., 1986; *Wunderlich et al*., 2013]. We suggest that NO_3^--NO_2^- interconversion across NXR results in expression of the equilibrium N isotope effect between NO_3^- and NO_2^-, which would explain the very low values of NO_2^- $\delta^{15}N$ that we calculate for the Southern Ocean surface. Moreover, differences in estimates of the assimilation isotope effects between $NO_3^- + NO_2^-$ and NO_3^--only data suggest that the intensity of NO_3^--NO_2^- interconversion is linked to the seasonal deepening of the mixed layer, suggesting a role for nitrifiers entrained from the dark T_{min} layer into the sunlit surface mixed layer. Enzyme-level interconversion of NO_3^- and NO_2^- is a new complication in our understanding of the marine N cycle. This process has the potential to be important in the many oceanographic environments where NO_2^- oxidizers can be transported across light or chemical gradients into waters with conditions unfavorable for NO_2^- oxidation.

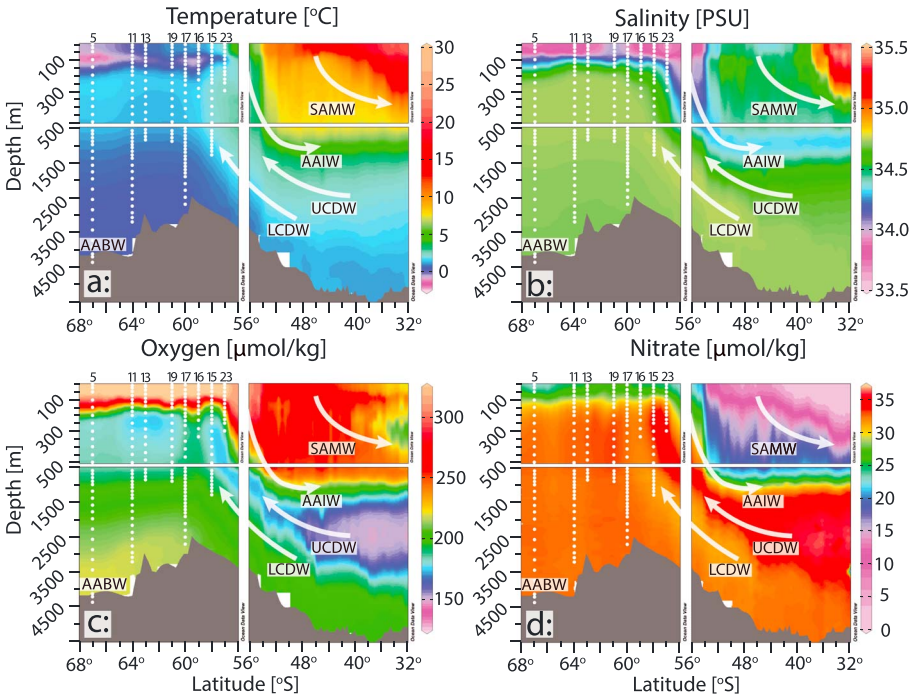

Figure 1. (a) Temperature (°C), (b) salinity (psu, practical salinity unit), (c) oxygen concentration (µmol/kg), and (d) NO_3^- concentration (µmol/kg) along 150°W. White dots show the locations of samples analyzed in this study, with station number given at the top of each profile. UCDW: Upper Circumpolar Deep Water; LCDW: Lower Circumpolar Deep Water; AABW: Antarctic Bottom Water; AAIW: Antarctic Intermediate Water; SAMW: Subantarctic Mode Water.

2. Methods

2.1. Cruise Track and Sample Collection

Seawater samples were collected during the 2014 U.S. Repeat Hydrography P16S cruise onboard the RVIB *Nathaniel B. Palmer*. From 20 March to 5 May, the cruise occupied a total of 90 stations from 67°S to 15°S along 150°W, and hydrographic information for each cast was collected from a Sea-Bird Electronics CTD. Water samples were collected every 25 to 50 m in the surface ocean and every 100 to 400 m at depth. The onboard science crew analyzed the samples for the concentrations of major nutrients, and measurements are presented here in their reported units.

The samples analyzed in this study were collected from eight stations between 57°S and 67°S (Figure 1, white circles). While some sampled profiles extended to the ocean floor, others were sampled only through the upper water column. Seawater was collected in 50 mL bottles that were rinsed three times with sample prior to filling and were frozen at −20°C within 2 h of collection. Inserts were added to the frozen sample bottles within 1 week of freezing. Initial isotopic analysis revealed that some of the collected samples were depleted in NO_3^- by as much as 50% of their shipboard-measured concentrations. Refractometer testing indicated that these samples also had reduced salinity, with measured-to-reported salinity ratios of 50–100%. The NO_3^- and salinity ratios fall close to a 1:1 line and suggest a linear relationship between salt loss and NO_3^- loss. These observations are consistent with the loss of brine, which likely formed and escaped when the sample froze in storage. To adjust for this brine loss, we measured the salinity of each sample and used regression lines to generate an estimate of actual NO_3^- concentration, which was then used to calculate the desired injection volume for our mass spectrometer measurements (see below). While our data set may be compromised modestly by this brine loss and associated variations in the volume of sample injections, inspection of the data for correlations between brine loss and isotopic composition yielded no compelling trends (supporting information Text S1 and Figure S1). Here we report NO_3^- concentrations as measured at sea, not the compromised concentrations in our sample bottles.

2.2. Isotopic Analysis of NO_3^- + NO_2^- and NO_3^--Only

NO_3^- $\delta^{15}N$ and $\delta^{18}O$ were measured using the denitrifier method, in which bacteria lacking an active nitrous oxide (N_2O)-reductase quantitatively convert seawater NO_3^- to N_2O gas [*Sigman et al.*, 2001; *Casciotti et al.*, 2002]. Additionally, the denitrifier method converts any NO_2^- in the sample to N_2O, which can confound interpretations of measured $\delta^{15}N$ and $\delta^{18}O$. NO_2^- in seawater affects measurements of $\delta^{18}O$ because, during bacterial conversion, NO_2^- loses a smaller fraction of O atoms than NO_3^- as the two N species are converted to N_2O (3/4 in NO_2^- versus 5/6 in NO_3^-). The isotopic impact of such differential O loss is that N_2O generated from NO_2^- has a $\delta^{18}O$ that is ~25‰ lower than N_2O produced from NO_3^- with the same initial $\delta^{18}O$ [*Casciotti et al.*, 2007], implying that our measured values systemically underestimate the true $\delta^{18}O$ of NO_3^- + NO_2^-. To correct for this methodological bias, we increased the measured $\delta^{18}O$ of NO_3^- + NO_2^- by the product of 25‰ and the fraction of NO_2^- in each sample ([NO_2^-]/[NO_3^- + NO_2^-]); the magnitude of this correction ranges from 0.00 to 0.31‰. It is important to note that this correction only applies to $\delta^{18}O$, not to $\delta^{15}N$, and that the magnitude of the correction is much smaller than the NO_3^- $\delta^{18}O$ difference between the surface ocean and deep ocean. Lastly, uncertainty in the exact correction factor, here taken as 25‰, is insufficient to explain the signals identified and discussed in the interpretation below. All further references to NO_2^- effects refer to the isotopic signal of NO_2^- in the water column and not to this methodological correction.

In order to isolate the NO_3^--only isotopic signal, all samples with detectable NO_2^- (concentrations ≥0.01 μmol/kg) were treated with sulfanilamide prior to analysis with the denitrifier method. During treatment, 200 μL of 1% sulfanilamide in 10% HCl were added per 10 mL of sample or standard and left for 7–10 min. 90–100 μL of 2 M NaOH was then added to increase sample pH to 6–8, as measured using pH indicator strips. This sulfanilamide-based protocol was undertaken as part of a methodological comparison with the sulfamic acid-based protocol of *Granger and Sigman* [2009]. The method comparison showed extremely similar results for the two protocols, for samples both with and without NO_2^-, consistent with prior testing of nitrite-spiked nitrate reference solutions [*Weigand et al.*, 2016]. Hereafter, the results from our samples and their NO_2^--removed counterparts are always distinguished because the presence or absence of NO_2^- is central to the discussion. We use "NO_3^--only" to refer to samples treated for NO_2^- removal or samples without any reported NO_2^-, while "NO_3^- + NO_2^-" refers to the original (untreated) sample. NO_3^--only and NO_3^- + NO_2^- plotted for deep samples without any reported NO_2^- represent the same measurements of untreated samples.

The isotopic composition of N_2O was measured by gas chromatography-isotope ratio mass spectrometry using a purpose-built online N_2O extraction and purification system and Thermo MAT 253 mass spectrometer [*Weigand et al.*, 2016]. Seawater solutions of the international NO_3^- reference materials IAEA-NO3 and USGS34 as well as gaseous injections from an in-house N_2O tank were run in parallel throughout the run, interspersed among the samples. Vials containing bacteria but no injected sample were also included in every batch to constrain bacterial blanks, and we conducted both within-batch and between-batch replications. On average, every sample was measured four times, and we report the simple average of the replicate measurements. The $\delta^{15}N$ and $\delta^{18}O$ of NO_3^- + NO_2^- was measured in 184 samples, and the $\delta^{15}N$ and $\delta^{18}O$ of NO_3^--only was measured in 88 samples. The pooled standard deviation of replicate sample measurements was 0.05‰ for $\delta^{15}N$ and 0.14‰ for $\delta^{18}O$ ($n = 272$). There was no significant difference in reproducibility between samples treated with sulfanilamide and their untreated counterparts. For an in-house seawater sample from the deep North Pacific that was measured two to three times in each run, the standard deviation was 0.04‰ for $\delta^{15}N$ and 0.12‰ for $\delta^{18}O$ ($n = 94$).

3. Results

3.1. Hydrography

Major water masses are identified from temperature, salinity, oxygen, and NO_3^- concentration (Figure 1). Upper Circumpolar Deep Water (UCDW) is characterized by high NO_3^- and low oxygen concentrations, properties typically associated with the remineralization of sinking organic matter in the middepths of the low-latitude Indo-Pacific. While UCDW upwells in the Open Antarctic Zone (OAZ) north of the Southern Antarctic Circumpolar Current Front (SACCF), Lower Circumpolar Deep Water (LCDW) upwells farther south

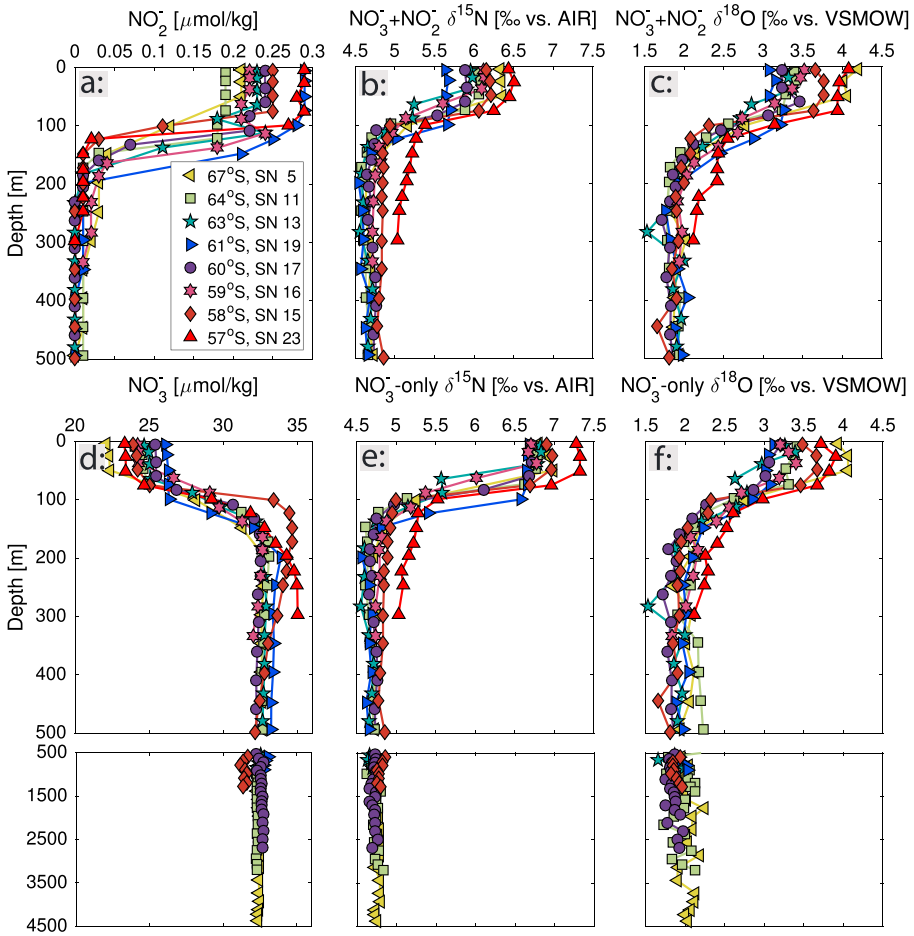

Figure 2. Depth profiles of (a) NO_2^- concentration, (b) $NO_3^- + NO_2^-$ $\delta^{15}N$, (c) $NO_3^- + NO_2^-$ $\delta^{18}O$, (d) NO_3^- concentration, (e) NO_3^--only $\delta^{15}N$, and (f) NO_3^--only $\delta^{18}O$. Note the different vertical scales between the first two rows of panels and the third row of panels.

within the Polar Antarctic Zone (PAZ). LCDW is relatively saline due to its incorporation of North Atlantic Deep Water (NADW) and is depleted in NO_3^- and enriched in oxygen relative to UCDW. Three stations in this analysis are in the OAZ between the Antarctic Polar Front (APF) and the SACCF, and five stations are in the PAZ south of the SACCF. Antarctic Bottom Water (AABW) is characterized by cold temperatures and high oxygen concentrations, which result from its recent contact with the surface and the high solubility of oxygen at low temperatures. Finally, Antarctic Intermediate Water (AAIW) and Subantarctic Mode Water (SAMW) are nutrient-rich, low-salinity water masses that form near the APF and the Subantarctic Front (SAF), respectively [*Orsi et al*., 1995], and provide nutrients to the low-latitude upper ocean [*Sarmiento et al*., 2004].

Several features of the Ross Sea Gyre between 57°S and 67°S are evident in the hydrographic data. The isolated remnant base of the winter mixed layer is identified as the T_{min} layer near 100 m, with the temperature minimum reaching between −2°C and −0.5°C (Figure 1a). The surface is significantly fresher than the underlying water, with the highest salinity for a given depth occurring between 62°S and 63°S (Figure 1b). The deeper isothermals and isohalines are domed, reflecting regional upwelling associated with the core of the cyclonic Ross Sea Gyre. There is also a region of greater oxygen depletion from 200 m to 350 m between 60°S and 64°S where oxygen concentrations are less than 180 μmol/kg (Figure 1c); the same region is characterized by a maximum in NO_3^- concentration (Figure 1d). Mixed layer depths for each station were determined by visually inspecting profiles of potential density for rapid increases in density relative to the average of the surface ocean. Mixed layer depths range from 58 m to 81 m, with the deepest mixed layer occurring at the station in the core of the gyre.

3.2. Isotopic Impact of NO_2^- Removal

Onboard nutrient analysis revealed NO_2^- concentrations less than 0.01 μmol/kg in samples collected below 300 m and concentrations ranging from 0.19–0.29 μmol/kg in the mixed layer, up to 1.3% of the combined $NO_3^- + NO_2^-$ pool (Figure 2a). Despite the small fractional contribution of NO_2^- to the $NO_3^- + NO_2^-$ pool, removing NO_2^- altered $\delta^{15}N$ by −0.1‰ to 1.0‰; that is, it tended to raise $\delta^{15}N$, with larger changes observed in samples with higher NO_2^- concentrations (Figures 2b and 2e). Removing NO_2^- altered $\delta^{18}O$ by −0.4‰ to 0.3‰ but without a clear tendency (Figures 2c and 2f) (supporting information Text S2 and Figure S2).

3.3. Major Isotopic Signals in the Water Column

At all stations, the $\delta^{15}N$ and $\delta^{18}O$ of NO_3^- are quite uniform in the deeper water column (Figure 2, third row of panels). Below 1000 m, where there is no detectable NO_2^-, NO_3^- $\delta^{15}N$ is 4.7 ± 0.0‰ and NO_3^- $\delta^{18}O$ is 2.0 ± 0.1‰ (1σ, $n = 46$). In the upper 200 m, the dominant signal is a rise in both $\delta^{15}N$ and $\delta^{18}O$ (Figures 2b, 2c, 2e, and 2f) coincident with the decrease in NO_3^- concentration (Figure 2d). The largest changes in all three parameters occur from below 200 m to above 50 m, where the mean NO_3^- concentration decreases from 32.6 ± 0.6 μmol/kg to 24.3 ± 1.2 μmol/kg. For $NO_3^- + NO_2^-$, the mean $\delta^{15}N$ and $\delta^{18}O$ increase from 4.7 ± 0.1‰ to 6.1 ± 0.2‰ and from 1.9 ± 0.1‰ to 3.5 ± 0.3‰, respectively; for NO_3^--only, the mean $\delta^{15}N$ and $\delta^{18}O$ increase from 4.7 ± 0.1‰ to 6.8 ± 0.2‰ and from 1.9 ± 0.1‰ to 3.4 ± 0.3‰, respectively (1σ, $n = 118$ below 200 m, $n = 22$ above 50 m). In the upper 50 m, NO_3^- concentration and $\delta^{15}N$ are relatively constant, while $\delta^{18}O$ varies slightly but without a clear trend. The large changes in NO_3^- concentration and isotope ratios from the subsurface into the surface ocean are attributable to NO_3^- assimilation by phytoplankton, which removes nutrients and causes the $\delta^{15}N$ and $\delta^{18}O$ of the remaining NO_3^- to rise [*Wada and Hattori*, 1978; *Pennock et al*., 1996; *Waser et al*., 1998; *Needoba et al*., 2004]. We do not observe strong meridional trends in NO_3^- concentration or isotopic composition, but the stations nearest to 61°S are consistently characterized by higher NO_3^- concentrations and lower NO_3^- $\delta^{15}N$ and $\delta^{18}O$. This is likely due to the proximity of these stations to the core of the Ross Sea Gyre, where upwelling is expected to be strongest.

3.4. Non-Rayleigh Dynamics and Estimation of Isotope Effects

In most profiles, NO_3^- $\delta^{15}N$ and $\delta^{18}O$ resemble LCDW at depth, consistent with their position south of the SACCF, while the northernmost stations 15 (58°S) and 23 (57°S) transition upward from LCDW to UCDW before the T_{min} is reached (Figure 3). According to the Rayleigh model, the $\delta^{15}N$ and $\delta^{18}O$ of NO_3^- versus $\ln(NO_3^-)$ should fall along linear trends connecting the subsurface water NO_3^- source, either UCDW or LCDW, with the surface samples. However, in all profiles the $\delta^{15}N$ of the T_{min} layer falls well below the linear trend defined by deeper and shallower NO_3^- (Figure 3, dashed black box indicating the concave-up "kink"), except for at station 15 (58°S) where samples from the T_{min} layer resemble underlying deep water. No comparable nonlinearity is observed for $\delta^{18}O$. Plots of the depth profiles in Rayleigh space are thus consistent with previous observations of non-Rayleigh behavior for NO_3^- samples in the remnant of the winter mixed layer [*Sigman et al*., 1999; *DiFiore et al*., 2010; *Smart et al*., 2015].

As a result of this non-Rayleigh behavior, we estimate larger N and O isotope effects for NO_3^- assimilation, $^{15}\varepsilon$ and $^{18}\varepsilon$, respectively, when taking the linear trend connecting the mixed layer samples with samples in the T_{min} than when regressing against full depth profiles. Because the T_{min} layer is thought to represent the initial concentration and isotopic composition of NO_3^- in the summertime surface [*Altabet and Francois*, 2001], regressions through the T_{min} likely yield the best approximation for the isotope effect of NO_3^- assimilation over a single season [*DiFiore et al*., 2010]. For $NO_3^- + NO_2^-$ samples, estimates of $^{15}\varepsilon$ calculated from regressions on samples from the surface to the core of the T_{min} layer range from 4.8 ± 0.3‰ to 6.1 ± 0.4‰, and estimates of $^{18}\varepsilon$ range from 2.5 ± 1.5‰ to 5.6 ± 0.7‰. For NO_3^--only samples, estimates of $^{15}\varepsilon$ range from 6.9 ± 0.4‰ to 11.7 ± 1.0‰, and estimates of $^{18}\varepsilon$ range from 2.5 ± 0.8‰ to 5.4 ± 0.7‰ (supporting information Text S3 and Figure S3). These cited ranges exclude station 15 (58°S), where sampled T_{min} water was nearly identical to underlying deep water in nitrate $\delta^{15}N$ and concentration and thus did not capture the characteristic $\delta^{15}N/\ln(NO_3^-)$ relationship of the temperature minimum layer.

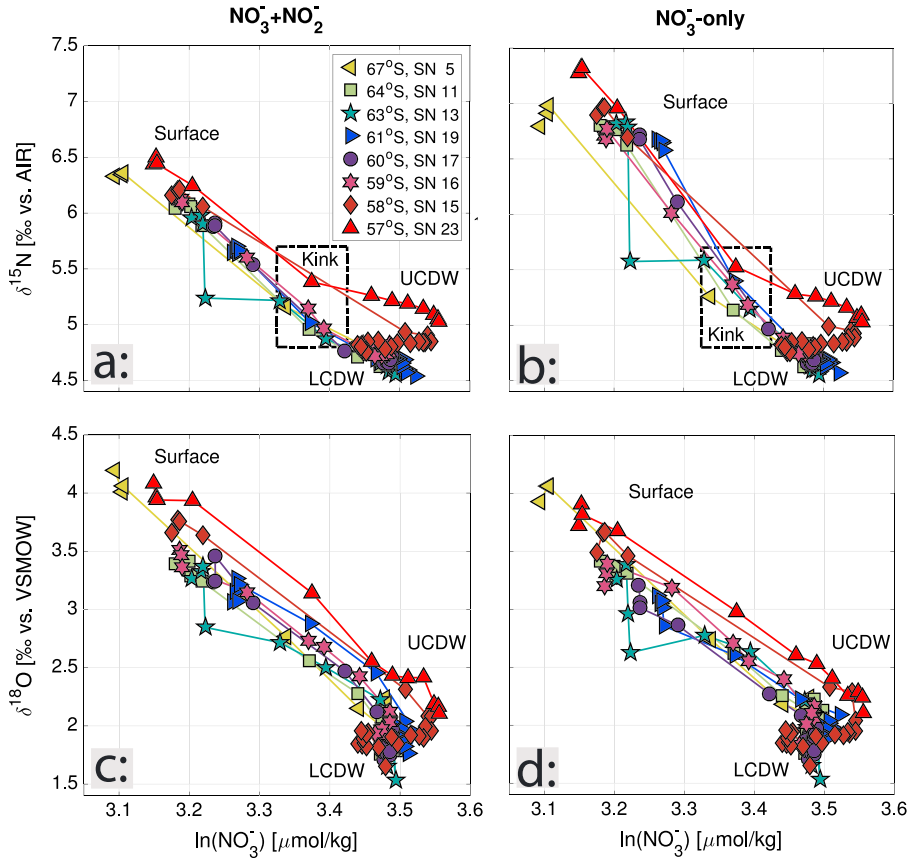

Figure 3. The $\delta^{15}N$ and $\delta^{18}O$ of $NO_3^- + NO_2^-$ and NO_3^--only data in Rayleigh space. Except for station 15, all stations show a concave-up $\delta^{15}N$ "kink" at the T_{min} layer (dashed black box), where NO_3^- $\delta^{15}N$ is lower for its concentration than the Rayleigh model predicts [*Sigman et al.*, 1999; *DiFiore et al.*, 2010]. No corresponding feature is seen in $\delta^{18}O$. Values do not change substantially when plotted against $\ln(NO_3^- + NO_2^-)$ instead of $\ln(NO_3^-)$.

4. Discussion

4.1. Observed $\delta^{15}N$ and $\delta^{18}O$ in $NO_3^- + NO_2^-$ and NO_3^--Only Samples

4.1.1. $NO_3^- + NO_2^-$ $\delta^{15}N$ and $\delta^{18}O$

In the absence of other processes, the nearly equal N and O isotope effects of NO_3^- assimilation would cause surface NO_3^- $\delta^{15}N$ and $\delta^{18}O$ to increase in parallel [*Granger et al.*, 2004, 2008, 2010; *Karsh et al.*, 2012, 2014]. Graphically, NO_3^- assimilation causes the $\delta^{15}N$ and $\delta^{18}O$ of NO_3^- to rise along a 1:1 slope in $\delta^{18}O$ versus $\delta^{15}N$ space. Below the T_{min}, $NO_3^- + NO_2^-$ samples show a uniform difference between $\delta^{15}N$ and $\delta^{18}O$ of ~3‰ (Figure 4a), consistent with previous Southern Ocean measurements [*Rafter et al.*, 2013; *Smart et al.*, 2015]. In the T_{min}, $NO_3^- + NO_2^-$ samples fall slightly above the 1:1 line in $\delta^{18}O$ versus $\delta^{15}N$ space, reflecting the decrease in NO_3^- $\delta^{15}N$ relative to $\ln(NO_3^-)$ within the T_{min} layer (i.e., the kink). This feature has been observed previously in winter data from the Atlantic sector of the AZ and is hypothesized to result from the remineralization of low-$\delta^{15}N$ N remaining in the mixed layer at the end of the summer [*Smart et al.*, 2015]. Moving into the surface ocean, the difference between $\delta^{15}N$ and $\delta^{18}O$ remains constant as the N and O isotope systems evolve in approximately the 1:1 fashion expected from NO_3^- assimilation acting alone. This 1:1 evolution continues until, in the surface samples, $\delta^{18}O$ changes slightly in some profiles.

4.1.2. NO_3^--Only $\delta^{15}N$ and $\delta^{18}O$

For the NO_3^--only samples, $\delta^{15}N$ and $\delta^{18}O$ show the same uniform difference of ~3‰ below the T_{min} layer that is observed in the $NO_3^- + NO_2^-$ data (Figure 4b). Likewise, in NO_3^--only as for $NO_3^- + NO_2^-$, $\delta^{15}N$ rises less than $\delta^{18}O$ from depth into the T_{min} layer. However, into the surface mixed layer, $NO_3^- + NO_2^-$ $\delta^{15}N$ and NO_3^--only $\delta^{15}N$ diverge. For the NO_3^--only data, $\delta^{15}N$ increases relative to $\delta^{18}O$ such that the shallowest samples fall below the 1:1 line extending from deep NO_3^-. Such a large increase in $\delta^{15}N$ relative to $\delta^{18}O$

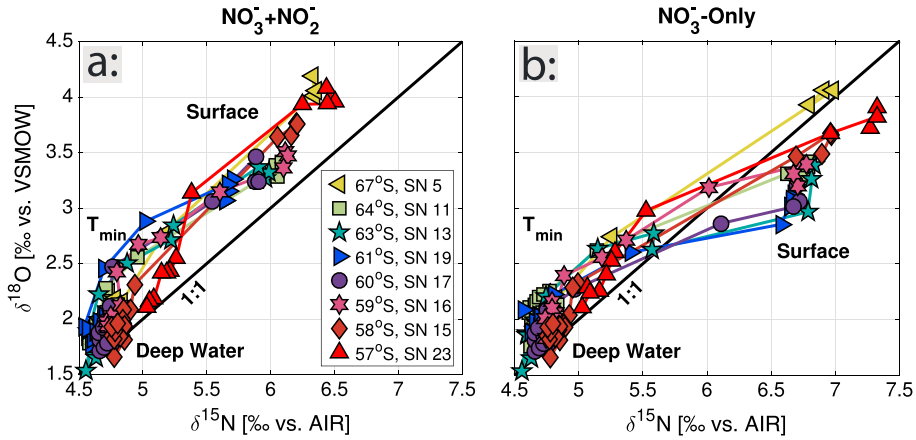

Figure 4. Cross plots of (a) $NO_3^- + NO_2^-$ and (b) NO_3^--only $\delta^{18}O$ against $\delta^{15}N$.

has not been observed previously. Moreover, the observations of both the 1:1 evolution of $NO_3^- + NO_2^-$ from the T_{min} into the surface and the larger increase in $\delta^{15}N$ relative to $\delta^{18}O$ for NO_3^--only are inconsistent with the expected results from previously described Southern Ocean dynamics.

4.2. Estimated and Predicted NO_2^- $\delta^{15}N$ and $\delta^{18}O$

4.2.1. Anomalously Low $\delta^{15}N$ of NO_2^- Derived Through Mass Balance

The $\delta^{15}N$ of NO_3^--only samples is higher than that of the $NO_3^- + NO_2^-$ samples, indicating a low $\delta^{15}N$ for NO_2^- relative to NO_3^-. The $\delta^{15}N$ of NO_2^- was calculated using an isotope mass balance, with error propagation derived from a Monte Carlo simulation. For each sample, we adjusted the reported concentration of NO_3^- and NO_2^-, as well as the measured values of $\delta^{15}N$ and $\delta^{18}O$, by values drawn randomly from normal distributions with characteristic standard deviations. In accordance with estimates of accuracy and precision derived from shipboard measurements of the Reference Materials for Nutrients in Seawater, the standard deviation was 0.21 μmol/kg for the NO_3^- distribution and 0.006 μmol/kg for the NO_2^- distribution. The standard deviation was 0.05‰ for $\delta^{15}N$ in untreated samples and 0.04‰ for $\delta^{15}N$ in treated samples, reflecting the pooled standard deviations of replicate measurements across our entire data set. After shifting each term in the mass balance equation, we recalculated NO_2^- $\delta^{15}N$ 100,000 times, and here we report the standard deviation of the resulting distribution as the uncertainty in NO_2^- $\delta^{15}N$ for each sample. The uncertainties in average NO_2^- $\delta^{15}N$ are given as the standard deviation of the constituent NO_2^- $\delta^{15}N$ values. Excluding samples with NO_2^- concentrations less than 0.10 μmol/kg, for which uncertainty in the calculation is highest, NO_2^- $\delta^{15}N$ ranges from -91 ± 18‰ to -6 ± 22‰, with an average value of -58 ± 52‰ (2σ, $n = 55$; Figure 5). NO_2^- $\delta^{15}N$ is depth dependent, with an average value above 90 m of -69 ± 33‰ (2σ, $n = 41$) that is lower than the value below 90 m of -24 ± 38‰ (2σ, $n = 14$; Figure 5, grey bar). In addition, the surface NO_2^- $\delta^{15}N$ is significantly lower than that calculated by *Smart et al.* [2015] for the Atlantic sector of the Antarctic Zone; using a similar approach, they estimated NO_2^- $\delta^{15}N$ to range from -40‰ to -20‰ in the winter mixed layer.

4.2.2. NO_2^- $\delta^{15}N$ Predicted From NH_4^+ and NO_2^- Oxidation and Assimilation

We first consider a mechanism suggested previously to explain observations of low-$\delta^{15}N$ NO_2^- in samples from the wintertime Atlantic AZ. *Lourey et al.* [2003] report that the $\delta^{15}N$ of surface suspended particulate nitrogen (PN) in the Pacific AZ decreases from ~0‰ to ~ −5‰ from early to late summer, an observation best explained as reflecting an increase in the assimilation of regenerated N, predominantly NH_4^+ [*Fawcett et al.*, 2011, 2014]. Relative to NO_3^-, NH_4^+ is low in $\delta^{15}N$ because of the net isotopic fractionation imparted by zooplankton metabolism and excretion [*Checkley and Miller*, 1989] and by the bacterial degradation of PN [*Lehmann et al.*, 2002]. At the end of the summer, the combined NH_4^+ and organic N pool in the AZ mixed layer will thus be low in $\delta^{15}N$ [*Lourey et al.*, 2003].

Simplistically, there are two possible fates for NH_4^+ in surface waters: assimilation by phytoplankton or oxidation to NO_2^- by nitrifying bacteria and archaea (i.e., the first step of nitrification). Nitrifier activity has been found to be inhibited by light [*Vanzella et al.*, 1989; *Guerrero and Jones*, 1996], although it may not be

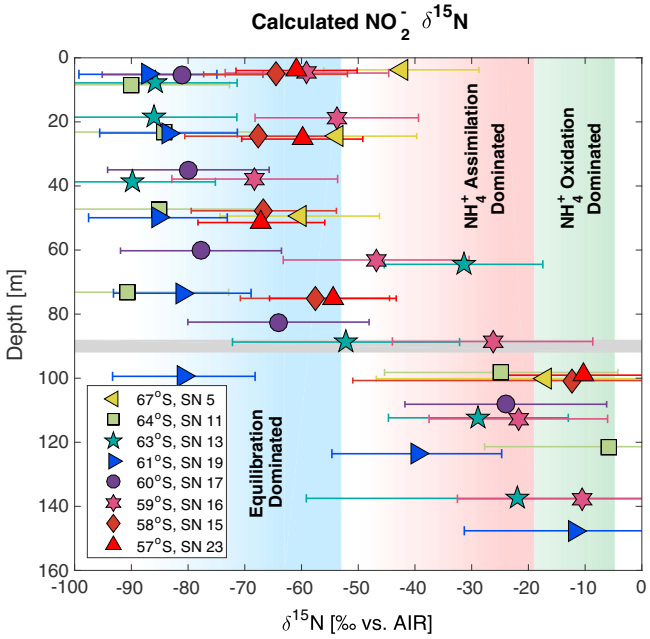

Figure 5. NO_2^- $\delta^{15}N$ with 2σ error for samples with NO_2^- concentrations greater than 0.10 μmol/kg. Predicted values for a system dominated by NH_4^+ oxidation are shown in green, a system dominated by NH_4^+ assimilation in red, and accounting for NO_3^--NO_2^- equilibration in blue. The fading of the shaded regions at lower $\delta^{15}N$ indicates the influence of net NO_2^- oxidation. The grey bar at 90 m separates surface and deep values of NO_2^- $\delta^{15}N$.

completely halted [*Ward*, 2005]. Coupled with the significant competitive advantage that phytoplankton have over nitrifiers for NH_4^+ [*Ward*, 1985; *Smith et al*., 2014], this typically leads to NH_4^+ oxidation being restricted to the dark waters below the photic zone and NH_4^+ assimilation dominating in surface waters. However, in the late summer AZ, the deepening mixed layer results in a decrease in the mean light level experienced by mixed layer organisms, potentially leading to the co-occurrence of NH_4^+ assimilation and nitrification. In this case, the $\delta^{15}N$ of the produced upper ocean NO_2^- depends on the relative rates of NH_4^+ assimilation and NH_4^+ oxidation. At the low NH_4^+ concentrations typical of AZ surface waters [*Gordon et al*., 2000], the isotope effect of NH_4^+ assimilation is expected to be near 0‰ [*Hoch et al*., 1992; *Liu et al*., 2013]. By contrast, the NH_4^+ oxidation isotope effect is thought to be 14–19‰ across a broader range of ammonium concentrations [*Casciotti et al*., 2003]. Assuming a starting NH_4^+ $\delta^{15}N$ of −5‰ in the late summer AZ surface [*Lourey et al*., 2003], if most of the NH_4^+ is oxidized and only a small fraction is assimilated, despite the substantial isotope effect of NH_4^+ oxidation, the $\delta^{15}N$ of the NO_2^- produced by oxidation will approximate the $\delta^{15}N$ of the NH_4^+ source, −5‰. Conversely, if assimilation is the dominant process and only a small fraction of the available NH_4^+ is oxidized, the NH_4^+ oxidation isotope effect will lower the $\delta^{15}N$ of NO_2^- produced by oxidation to roughly −24‰ to −19‰.

The NO_2^- produced from NH_4^+ oxidation can either be assimilated with an isotope effect of ~0‰ [*Waser et al*., 1998] or be oxidized to NO_3^- with an inverse isotope effect of −12.8‰ [*Casciotti*, 2009]. If most of the NO_2^- is assimilated, the $\delta^{15}N$ of the unassimilated NO_2^- will remain effectively unchanged, at either −5‰ or in the range of −24‰ to −19‰. If the regime is dominated by NO_2^- oxidation, however, the inverse isotope effect will have a significant impact. If ~63% of the available NO_2^- is oxidized, the unoxidized NO_2^- will be left with a $\delta^{15}N$ of −17.8‰ for the system dominated by NH_4^+ oxidation (Figure 5, green shading) or −36.8‰ for the system dominated by NH_4^+ assimilation (Figure 5, red shading). Although the minimum NO_2^- $\delta^{15}N$ suggested by the scenarios outlined above is very low, it is still significantly higher than many of the NO_2^- $\delta^{15}N$ values calculated here for the AZ surface.

Furthermore, NH_4^+ oxidation and NH_4^+ assimilation cannot explain our observation that $NO_3^- + NO_2^-$ $\delta^{15}N$ and $\delta^{18}O$ evolve along an approximately 1:1 trend while NO_3^--only samples exhibit elevated $\delta^{15}N$ relative to $\delta^{18}O$. The generation of a low-$\delta^{15}N$ NO_2^- pool would cause a larger discrepancy from expectations in the $\delta^{15}N$ to $\delta^{18}O$ relationship of $NO_3^- + NO_2^-$ than of NO_3^--only, with the latter only impacted if there is some oxidation of NO_2^- to NO_3^-. Instead, we observe the opposite situation, in which the expected 1:1 relationship between $\delta^{15}N$ and $\delta^{18}O$ is seen in the $NO_3^- + NO_2^-$ data but we observe a substantial deviation from expectations in the NO_3^--only data.

4.2.3. NO_2^- $\delta^{18}O$ Altered During Storage

Abiotic oxygen exchange between NO_2^- and H_2O during sample storage very likely removed any relevant oceanographic information from the NO_2^- $\delta^{18}O$ of our samples [*Casciotti et al*., 2007; *Casciotti and McIlvin*,

2007] but does not appear to have significantly altered the $\delta^{18}O$ of $NO_3^- + NO_2^-$. The incorporation of O from H_2O likely had only minor impacts on the $\delta^{18}O$ of $NO_3^- + NO_2^-$ because the $\delta^{18}O$ of NO_2^- equilibrated with H_2O is roughly comparable to the $\delta^{18}O$ of partially consumed NO_3^- [*Buchwald and Casciotti*, 2013], an interpretation that is supported by the observation that $\delta^{18}O$ is very similar between $NO_3^- + NO_2^-$ and NO_3^--only analyses (Figure 2). While the $\delta^{18}O$ of NO_2^- in our samples does not contain relevant information, the $\delta^{18}O$ of NO_3^- may record previous interactions with the NO_2^- pool, as described below.

4.3. Evidence for Enzyme-Level NO_3^--NO_2^- Interconversion

4.3.1. Nitrogen Isotopes in NO_3^- and NO_2^-

Interconversion of NO_3^- and NO_2^- at an intracellular/periplasmic, enzyme scale can explain both the positive deviation of mixed layer NO_3^--only $\delta^{15}N$ relative to $\delta^{18}O$ (Figure 4b) and the extremely low $\delta^{15}N$ of surface NO_2^- (Figure 5). Such interconversion would lead to expression of the N equilibrium isotope effect between NO_3^- and NO_2^-, which would enrich NO_3^- in ^{15}N and deplete NO_2^- in ^{15}N [*Casciotti*, 2009] while not altering the combined $\delta^{15}N$ of the $NO_3^- + NO_2^-$ present in the summer mixed layer. Thus, the $NO_3^- + NO_2^-$ data would evolve according to expectations for NO_3^- assimilation, but because NO_2^--removed samples contain only the NO_3^- enriched in ^{15}N by interconversion, NO_3^--only $\delta^{15}N$ would increase more rapidly than does $NO_3^- + NO_2^-$ $\delta^{15}N$. Likewise, because NO_2^- is depleted in ^{15}N during interconversion, we would calculate low values for NO_2^- $\delta^{15}N$. The impact of interconversion on the $\delta^{18}O$ of NO_3^- and NO_2^- is complex, involving multiple processes and considerations, including the incorporation of oxygen from ambient H_2O during nitrification and abiotic exchange as well as the isotope effects of oxygen incorporation and loss [*Buchwald and Casciotti*, 2013]. As discussed below, the $\delta^{18}O$ in NO_3^- and NO_2^- does appear to be impacted by NO_3^--NO_2^- interconversion, with data indicating a $\delta^{18}O$ decline in both $NO_3^- + NO_2^-$ and NO_3^--only measurements.

Previous evidence for N isotopic equilibration between NO_3^- and NO_2^- includes a study by *Brunner et al.* [2013] wherein a large increase in NO_3^- $\delta^{15}N$ and a corresponding decrease in NO_2^- $\delta^{15}N$ was measured in cultures of anaerobic ammonia oxidizing (anammox) bacteria. These observations were interpreted to reflect N exchange and the expression of an equilibrium isotope effect between NO_3^- and NO_2^-, proposed to result from the reversibility of a biochemical reaction. One mechanism that could drive interconversion and N exchange involves the reversibility of the nitrite oxidoreductase (NXR) enzyme, which is used by some nitrifying organisms to oxidize NO_2^- to NO_3^- and which can also catalyze the reduction of NO_3^- to NO_2^- [*Sundermeyer-Klinger et al.*, 1984]. NXR is a membrane-associated enzyme with both cytoplasmic and periplasmic types, which occur in distinct groups of NO_2^--oxidizing bacteria [*Pester et al.*, 2014]. *Friedman et al.* [1986] undertook some of the initial work on the NXR enzyme, using ^{15}N- and ^{18}O-labeled NO_3^- and NO_2^- to demonstrate O transfer between NO_3^- and NO_2^- in cultures of nitrifying bacteria. *Wunderlich et al.* [2013] later used ^{18}O labeling to provide further evidence for O atom exchange among NO_3^-, NO_2^-, and H_2O in both natural populations of NO_3^--reducing microorganisms and pure cultures of NO_2^--oxidizing bacteria under anoxic conditions, which they attributed to the reversibility of NXR. It thus appears that the bidirectional NXR enzyme can catalyze the intracellular coupled oxidation of NO_2^- and reduction of NO_3^- to result in the expression of a NO_3^--NO_2^- equilibrium N isotope effect, without requiring net oxidation at either the scale of the enzyme or the organism [*Friedman et al.*, 1986; *Brunner et al.*, 2013; *Wunderlich et al.*, 2013].

When NO_2^- oxidation and NO_3^- reduction occur at the organismal scale, the enzymatic isotope effects of the two processes can be underexpressed due to substantial consumption of the substrate within the cells of nitrifiers and denitrifiers [e.g., *Kritee et al.*, 2012]. Thus, compensating NO_3^- reduction and NO_2^- oxidation by a consortium of nitrate reducers and nitrite oxidizers in an ocean water parcel are unlikely to approximate the equilibrium N isotope effect between NO_3^- and NO_2^-. Conversely, the full magnitude of the equilibrium N isotope effect can be captured when the coupled oxidation and reduction occurs intracellularly, where the NO_2^- oxidoreductase enzyme operates on an intracellular (or periplasmic) N pool composed of both NO_3^- and NO_2^-. The proposed intracellular coupling of NO_2^- oxidation and NO_3^- reduction thus would have a different isotopic impact from the counteraction of NO_2^- oxidation and NO_3^- reduction by distinct NO_2^--oxidizing and NO_3^--reducing organisms in an ocean water parcel.

Casciotti [2009] used vibrational partition functions to calculate an N equilibrium fractionation factor of 0.9454 at 24.85°C for the reaction $^{14}NO_2^- + {}^{15}NO_3^- \Leftrightarrow {}^{15}NO_2^- + {}^{14}NO_3^-$, corresponding to an inverse isotope

Table 1. Estimates of the Equilibrium N Isotope Effect Between NO_3^- and NO_2^- Using Four Different Sets of Molecular Vibrational Frequencies in ^{15}N and ^{14}N-bearing NO_3^- and NO_2^-[a]

	$T = 0$°C	$T = 24.85$°C	$T = 31$°C
	Southern Ocean	Standard Temperature	*Brunner et al.* [2013]
Walters and Michalski [2015]	−59.9‰	−52.9‰	−51.4‰
Casciotti [2009]	−61.7‰	−54.6‰	−53.0‰
Begun and Fletcher [1960]	−69.2‰	−61.2‰	−59.4‰
Spindel [1954]	−93.3‰	−83.0‰	−80.7‰

[a]Vibrational frequencies are for the aqueous phase in *Walters and Michalski* [2015] (averaging results from the B3LYP and EDF2 levels of theory), *Casciotti* [2009], and *Begun and Fletcher* [1960] but are unknown for *Spindel* [1954].

effect of −54.6‰. We extended this calculation to a range of temperatures for four different sets of reported molecular vibrational frequencies in ^{15}N and ^{14}N-bearing NO_3^- and NO_2^- (Table 1). The frequencies are derived from a combination of computational chemistry simulations [*Casciotti*, 2009; *Walters and Michalski*, 2015], empirical observations [*Spindel*, 1954; *Begun and Fletcher*, 1960], and calculations [*Spindel*, 1954]. The resulting estimates of the NO_3^--NO_2^- equilibrium isotope effect range from −83.0‰ to −52.9‰ at 24.85°C and from −93.3‰ to −59.9‰ at 0°C.

In their experiments incubating cultures of anammox bacteria at 31°C, *Brunner et al.* [2013] empirically derived a value for the NO_3^--NO_2^- equilibrium isotope effect of −60.5 ± 1‰. This value is very close to the theoretical value of −59.4‰ derived at this temperature from the vibrational frequencies of *Begun and Fletcher* [1960] but is significantly lower than the values of −51.4‰ and −53.0‰ predicted using the frequencies reported in *Walters and Michalski* [2015] and *Casciotti* [2009], respectively. The data from *Spindel* [1954] differ considerably from the other studies and are based on early calculations, so they are excluded from the remainder of this analysis. Details aside, there is still uncertainty in the magnitude of the NO_3^--NO_2^- equilibrium isotope effect, deriving largely from uncertainty in the different molecular vibrational frequencies of ^{15}N and ^{14}N-bearing NO_3^- and NO_2^-.

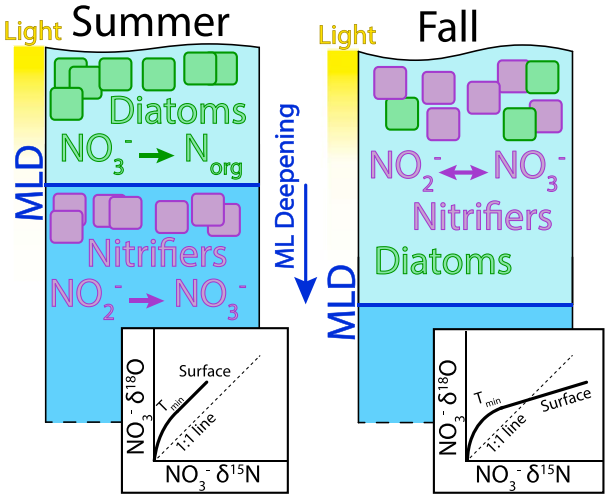

Figure 6. Proposed dynamics of interconversion of NO_3^- and NO_2^-. (left) During the summer, the surface ocean is thermally stratified. Diatoms, the dominant phytoplankton group in the Ross Sea region during the growing season [*Peloquin and Smith*, 2007], consume NO_3^- in the photic zone, while nitrifiers are largely restricted to the waters below the mixed layer. $\delta^{15}N$ and $\delta^{18}O$ of NO_3^- increase in a 1:1 relationship into the mixed layer as a result of nitrate assimilation. This relationship is preserved in the isotopic composition of the combined $NO_3^- + NO_2^-$. (right) As the mixed layer deepens into the fall and nitrifying organisms are entrained into the surface ocean, the reversible nitrite oxidoreductase enzyme catalyzes the oxidation of NO_2^- and the reduction of NO_3^-. Such a bidirectional reaction may allow for the expression of a large equilibrium N isotope effect, resulting in the production of extremely low-$\delta^{15}N$ NO_2^- and increasing NO_3^- $\delta^{15}N$ relative to NO_3^- $\delta^{18}O$, causing NO_3^--only depth profiles to deviate from the 1:1 line in $\delta^{18}O$ versus $\delta^{15}N$ space in the manner illustrated by the black curves.

In the Southern Ocean surface, the expression of an equilibrium isotope effect of −69.2‰ to −59.9‰ would generate NO_2^- $\delta^{15}N$ ranging from roughly −63‰ to −53‰; this range of NO_2^- $\delta^{15}N$ can be expected for a large range of initial (pre-equilibrated) NO_2^- $\delta^{15}N$ values, assuming a NO_3^- concentration of ~25 μmol/kg, a NO_2^- concentration of ~0.25 μmol/kg, and an initial NO_3^- $\delta^{15}N$ of ~6‰. The NO_2^- $\delta^{15}N$ values expected to result from equilibration with NO_3^- (Figure 5, blue shading) are in much better agreement with the observed values than are the predictions resulting from NH_4^+ and NO_2^- oxidation and assimilation. Even accounting for this equilibrium, however, some

samples have a lower NO_2^- $\delta^{15}N$ than expected. This observation is potentially explained by NO_2^- oxidation subsequent to the interconversion, which would further decrease NO_2^- $\delta^{15}N$ [*Casciotti*, 2009].

The $\delta^{15}N$ and $\delta^{18}O$ of $NO_3^- + NO_2^-$ and NO_3^--only from the wintertime AZ do not show signs of NO_3^--NO_2^- interconversion [*Smart et al.*, 2015]. Rather, *Smart et al.* [2015] observed deviations in both $NO_3^- + NO_2^-$ and NO_3^--only toward lower $\delta^{15}N$ relative to $\delta^{18}O$, which is a pattern that calls for the nitrification of low-$\delta^{15}N$ N. An intensive comparison of $NO_3^- + NO_2^-$ and NO_3^--only isotope data from the Sargasso Sea near Bermuda also showed no sign of NO_3^--NO_2^- interconversion in that subtropical gyre environment [*Fawcett et al.*, 2015]. Thus, while there are few comparisons of $NO_3^- + NO_2^-$ and NO_3^--only isotopic data across the global ocean, it appears that some aspect of the late summer/fall AZ mixed layer is important in leading to NO_3^--NO_2^- interconversion.

We suggest that the NO_3^--NO_2^- interconversion is encouraged by the deepening of the mixed layer in late March and early April. As the mixed layer deepens into the fall and erodes into the underlying T_{min} layer, where nitrifiers have presumably been active during the summer, some of these nitrifiers may be entrained from the T_{min} layer into the fall surface ocean. Upon exposure to elevated levels of light or other new conditions, the NO_2^- oxidizers may slow their activity, such that the unidirectional oxidation of NO_2^- to NO_3^- is reduced [*Vanzella et al.*, 1989]. Under these conditions, the bifunctional NXR enzyme may catalyze both the forward and back reactions, yielding the isotopic distribution expected from NO_3^--NO_2^- interconversion (Figure 6). Our hypothesis of NO_3^--NO_2^- interconversion in the Pacific AZ surface is supported by the rapid increase in NO_2^- $\delta^{15}N$ near the base of the mixed layer in each profile (Figure 5, grey bar), which suggests that the production of low-$\delta^{15}N$ NO_2^- is confined to the mixed layer, where light levels are highest.

Additional evidence for the scenario proposed in Figure 6 is the difference between the apparent isotope effects of NO_3^- assimilation derived from $NO_3^- + NO_2^-$ and NO_3^--only samples. If high-$\delta^{15}N$ N were shuttled into the NO_3^- pool, the apparent value of $^{15}\varepsilon$ in NO_3^--only data would increase and result in $^{15}\varepsilon_{NO3\text{-}only} > {}^{15}\varepsilon_{NO3+NO2}$ (Figure 7a, triangle). By this logic, the difference in $^{15}\varepsilon$ between NO_3^--only and $NO_3^- + NO_2^-$ can be taken as a measure of the degree of NO_3^--NO_2^- interconversion. In our data, the NO_3^--only samples at all stations yield estimates of $^{15}\varepsilon$ that are higher than those derived for $NO_3^- + NO_2^-$ samples (Figure 7b). This is best explained as resulting from the ^{15}N enrichment of NO_3^- relative to NO_2^- during interconversion. The difference in $^{15}\varepsilon$ between $NO_3^- + NO_2^-$ and NO_3^--only data, which we propose as a reflection of the intensity of interconversion, is strongly positively correlated with the depth of the mixed layer (Figure 7c). This may be because greater mixed layer deepening entrains more nitrifying organisms into the surface ocean, leading to greater NO_3^--NO_2^- interconversion. The highest intensity of interconversion occurs directly above the core of Ross Sea Gyre upwelling at station 19 (61°S), which we attribute to increased excavation of NO_2^- oxidizers from the T_{min} layer into surface waters due to strong Ekman upwelling and its tendency to yield faster mixed layer deepening in the late summer/fall.

In this framework, the lack of evidence for NO_3^--NO_2^- interconversion in the wintertime AZ [*Smart et al.*, 2015] can be explained by the low light of the ~175 m deep winter AZ mixed layer, which reduces inhibition of NO_2^- oxidation. While the Sargasso Sea has well-lit surface waters, the strength of density stratification and the net convergence of surface water in the subtropics work against the upward transport of nitrite oxidizers into those well-lit waters, explaining the lack of evidence for NO_3^--NO_2^- interconversion in the region [*Fawcett et al.*, 2015]. Given a general lack of complementary $NO_3^- + NO_2^-$ and NO_3^--only isotope data, it is unclear whether NO_3^--NO_2^- interconversion occurs in the midsummer AZ. While the deepening of the mixed layer would not apply to the early summer or midsummer, wind-driven upwelling (of ~3 m/month) may be adequate to drive some transport of nitrite oxidizers into the sunlit summer mixed layer and potentially lead to NO_3^--NO_2^- interconversion.

4.3.2. Oxygen Isotope Impacts of the Proposed Interconversion

Above, we noted that we observe an approximately 1:1 relationship between $\delta^{15}N$ and $\delta^{18}O$ in $NO_3^- + NO_2^-$ but an increase in $\delta^{15}N$ relative to $\delta^{18}O$ in NO_3^--only (Figure 4). When we look in greater detail, however, the $NO_3^- + NO_2^-$ data also show a discrepancy from the 1:1 $\delta^{15}N$-to-$\delta^{18}O$ relationship expected from nitrate assimilation acting alone (Figure 7a, circle) [*Granger et al.*, 2004, 2008, 2010; *Karsh et al.*, 2012, 2014]. Our

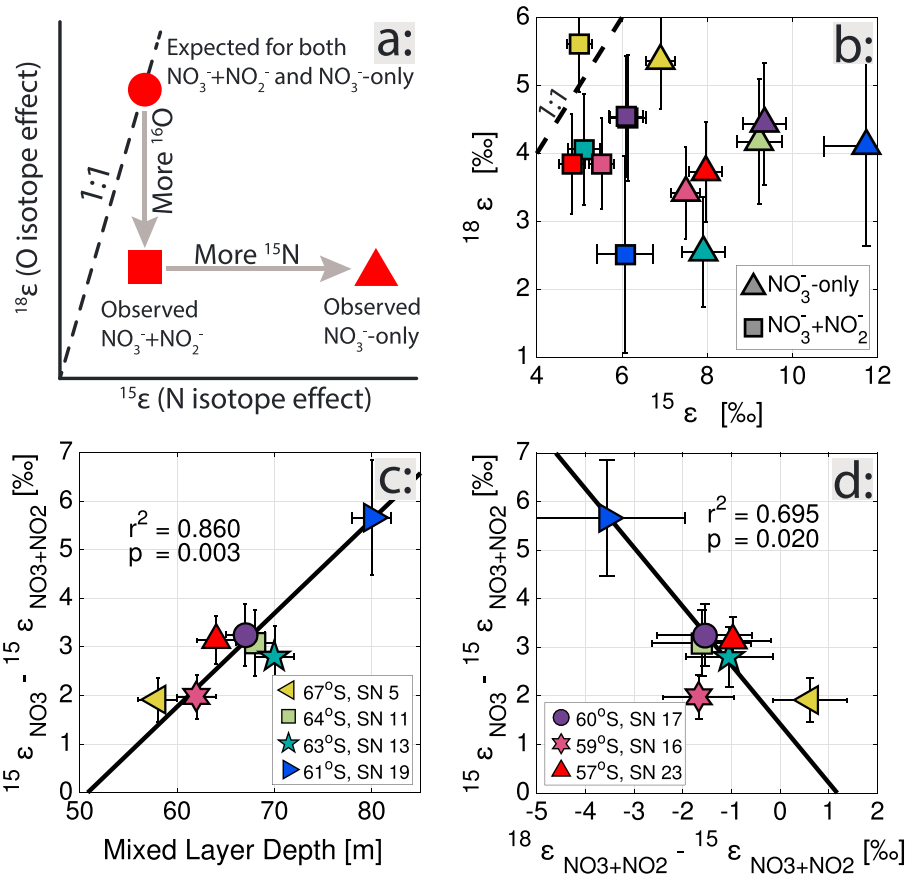

Figure 7. (a) Schematic showing how interconversion of NO_3^- and NO_2^- and the associated incorporation of O atoms from H_2O into either NO_3^- or NO_2^- may affect the apparent values of $^{15}\varepsilon$ and $^{18}\varepsilon$. (b) The $^{18}\varepsilon$ versus $^{15}\varepsilon$ for $NO_3^- + NO_2^-$ and NO_3^--only profiles. Note the different scales for $^{18}\varepsilon$ and $^{15}\varepsilon$. (c) The difference between $^{15}\varepsilon_{NO3\text{-}only}$ and $^{15}\varepsilon_{NO3+NO2}$, a proposed measure for the intensity of NO_3^--NO_2^- interconversion, is strongly correlated with mixed layer depth, consistent with mixed layer deepening entraining NO_2^- oxidizers into the surface ocean. (d) The apparent intensity of NO_3^--NO_2^- interconversion is also strongly inversely correlated with the offset in $\delta^{18}O$ of $NO_3^- + NO_2^-$ data from 1:1 expectations, consistent with the incorporation of water oxygen during the interconversion process. Plots exclude station 15 (58°S), where sampled T_{min} water was nearly identical to underlying deep water in nitrate $\delta^{15}N$ and concentration.

estimates of $^{18}\varepsilon$ from $NO_3^- + NO_2^-$ samples are up to 3.6‰ lower than the estimates of $^{15}\varepsilon$ at the same stations (Figure 7b), The implication of this observation is that low-$\delta^{18}O$ oxygen is introduced into either mixed layer NO_3^- or NO_2^- by NO_3^--NO_2^- interconversion, lowering the apparent value of $^{18}\varepsilon$ in $NO_3^- + NO_2^-$ such that $^{15}\varepsilon_{NO3+NO2} > {}^{18}\varepsilon_{NO3+NO2}$ (Figure 7a, square). Consistent with this view, the offset of $^{18}\varepsilon$ from $^{15}\varepsilon$ in the $NO_3^- + NO_2^-$ samples is inversely correlated with the difference in $^{15}\varepsilon$ between $NO_3^- + NO_2^-$ and NO_3^--only (Figure 7d), the latter having been proposed above as a reflection of the intensity of NO_3^--NO_2^- interconversion. The decrease in the $\delta^{18}O$ of $NO_3^- + NO_2^-$ may result from the incorporation of O atoms from ambient H_2O into either NO_2^- or NO_3^-, as NO_3^--NO_2^- interconversion will ensure that the $\delta^{18}O$ of NO_3^--only is lowered in either case. Indeed, estimates of $^{18}\varepsilon$ from NO_3^--only measurements are also lower than $^{15}\varepsilon$ from $NO_3^- + NO_2^-$ measurements (Figure 7b). While the O isotope systematics expected from the NO_3^--NO_2^- interconversion cannot easily be extracted from existing information on other processes (see supporting information Text S4), it appears that NO_3^--NO_2^- interconversion causes an underestimation of the O isotope effect of NO_3^- assimilation. Despite these observations, we emphasize that incorporation of low-$\delta^{18}O$ oxygen during NO_3^--NO_2^- interconversion can explain only a small portion of the offset of the NO_3^--only $\delta^{15}N$ and $\delta^{18}O$ data from 1:1 expectations (Figure 4b); most of this offset results from the increase in NO_3^--only $\delta^{15}N$ relative to $NO_3^- + NO_2^-$ $\delta^{15}N$.

4.4. Implications

4.4.1. Southern Ocean

The observed NO_3^--NO_2^- interconversion represents a previously unrecognized influence on nitrate N and O isotopic dynamics in the Southern Ocean. Our data indicate that this process can significantly alter the $\delta^{15}N$ and $\delta^{18}O$ of both NO_3^- and NO_2^-, whereas the two pools were previously thought to be isotopically related only through the kinetic isotope effects associated with NO_2^- oxidation and NO_3^- reduction. Moreover, in the sunlit upper ocean, vigorous interaction between NO_2^- and NO_3^- has generally not been expected, with the dominant relevant processes formerly thought to be assimilatory NO_3^- reduction followed quickly by NO_2^- reduction.

As described above, the existing data suggest that NO_3^--NO_2^- interconversion is important only in specific upper ocean environments. This study captured AZ conditions in the late summer and early fall, when the summertime nutrient uptake has essentially ended and the isotopic signal from interconversion is likely only minimally incorporated into sinking phytoplankton biomass. However, if the imprint of isotopic equilibration is preserved through the winter or redevelops early in the summer, the main pulse of phytoplankton biomass production, including that of diatoms, will incorporate it. This is relevant to paleoceanographic reconstructions of NO_3^- consumption using $\delta^{15}N$ data. The wintertime AZ shows no sign of the $\delta^{15}N$-to-$\delta^{18}O$ elevation in NO_3^--only that we observe in the late summer [*Smart et al*., 2015]. This implies that wintertime processes destroy the signal, most likely by dilution of the fall mixed layer NO_3^- with NO_3^- from the underlying T_{min}. However, as discussed above, NO_3^--NO_2^- interconversion may occur during summer high-growth periods; this will be critical to evaluate with new data.

4.4.2. Oxygen-Deficient Zones

A counterintuitive finding in the ocean's subsurface oxygen-deficient zones (ODZs), both from ^{15}N tracer studies [*Lipschultz et al*., 1990; *Füssel et al*., 2012; *Beman et al*., 2013; *Peng et al*., 2015] and natural abundance isotope observations [*Casciotti and McIlvin*, 2007; *Casciotti et al*., 2013; *Gaye et al*., 2013; *Buchwald et al*., 2015], is that NO_2^- appears to undergo oxidation to NO_3^- despite the lack of appropriate oxidants in the environment. In tracer studies, this has been shown through the addition of ^{15}N-labeled NO_2^- to seawater samples collected from suboxic zones and the subsequent detection of ^{15}N-labeled NO_3^- after incubation under anoxic conditions [*Füssel et al*., 2012; *Beman et al*., 2013; *Peng et al*., 2015]. In natural abundance studies, the same conclusion of NO_2^- oxidation is reached through the observation of a decoupling of NO_3^- $\delta^{15}N$ from NO_3^- $\delta^{18}O$ and of very low values of NO_2^- $\delta^{15}N$ relative to NO_3^- $\delta^{15}N$ in suboxic waters; these observations have been attributed to forcings from the combined isotope effects of NO_3^- reduction, NO_2^- reduction and oxidation, and anammox [*Casciotti and McIlvin*, 2007; *Casciotti*, 2009; *Casciotti et al*., 2013; *Gaye et al*., 2013; *Buchwald et al*., 2015; *Martin and Casciotti*, 2016]. Again, the perplexing aspect of interpretations suggesting NO_2^- oxidation in ODZ waters is the lack of appropriate oxidized species in the water column to serve as electron acceptors [*Buchwald et al*., 2015; *Peng et al*., 2015].

The subsurface ODZs are another candidate environment for NO_3^--NO_2^- interconversion, due to possible transport of NO_2^- oxidizers into these zones. Indeed, enzyme-level interconversion between NO_3^- and NO_2^- provides a straightforward explanation for the evidence from tracer studies of NO_2^- oxidation in ODZs. If NO_3^- and NO_2^- are able to interconvert without net oxidation due to biochemical reversibility, the high $^{15}N/^{14}N$ ratio of ^{15}N-labeled NO_2^- will appear in NO_3^- even when incubated under anoxic conditions. Thus, tracer study data can be explained without invoking net NO_2^- oxidation at either the enzyme or organism scale. We suggest that the results of such studies be reevaluated in the context of possible enzyme-level NO_3^--NO_2^- interconversion.

Enzyme-level NO_3^--NO_2^- interconversion also provides an alternative explanation for natural abundance isotopic patterns in ODZs that have been interpreted as evidence of organism-scale NO_2^- oxidation. The decoupling of NO_3^- $\delta^{15}N$ from NO_3^- $\delta^{18}O$ and the increase in NO_3^- $\delta^{15}N$ relative to NO_2^- $\delta^{15}N$ may both reflect the equilibrium isotope effect-driven partitioning of ^{15}N into NO_3^- and ^{14}N into NO_2^-. As ^{15}N is concentrated in NO_3^-, NO_3^- $\delta^{15}N$ increases, NO_2^- $\delta^{15}N$ decreases, and NO_3^- $\delta^{18}O$ changes. While the calculated values of NO_2^- $\delta^{15}N$ in our surface samples are lower than those observed in ODZs, this can be explained by net NO_2^- reduction in ODZs, which would act to increase NO_2^- $\delta^{15}N$ relative to our observations. We do not intend to suggest that the observed NO_3^-/NO_2^- $\delta^{15}N$ differences and the decoupling of $\delta^{15}N$ and $\delta^{18}O$ in and near ODZs are explained entirely by enzyme-level NO_3^--NO_2^- interconversion; NO_3^- and NO_2^-

reduction, organism-level net NO_2^- oxidation, and the various processes involved in anammox are all probably involved. Even regional N fixation may play a role in the decoupling of NO_3^- $\delta^{15}N$ and $\delta^{18}O$ in the ODZs [*Sigman et al*., 2005]. Nevertheless, NO_3^--NO_2^- interconversion may represent an important component process, especially at the ODZ boundaries.

5. Conclusions

We report $\delta^{15}N$ and $\delta^{18}O$ for $NO_3^- + NO_2^-$ and NO_3^--only in samples from eight depth profiles in the Pacific sector of the Southern Ocean's Antarctic Zone, collected in late March and early April. We find that the $\delta^{15}N$ and $\delta^{18}O$ of the combined $NO_3^- + NO_2^-$ pool increase roughly in parallel in accordance with expectations for NO_3^- assimilation, but NO_3^--only data show a strong elevation in $\delta^{15}N$ relative to $\delta^{18}O$ in the surface mixed layer. Differencing the measurements reveals that NO_2^- in the surface ocean is extremely low in $\delta^{15}N$, on average about −70‰ versus air. These observations are interpreted to reflect intracellular (cytoplasmic or periplasmic), enzyme-level interconversion between NO_3^- and NO_2^-, possibly mediated by biochemical reversibility of the nitrite oxidoreductase enzyme of NO_2^- oxidizing organisms entrained from the T_{min} layer into the sunlit mixed layer during the early phases of mixed layer deepening in the late summer. According to this interpretation, NO_3^--NO_2^- interconversion can be important where NO_2^- oxidizing organisms are transported into conditions that discourage NO_2^- oxidation; in the case of the late summer Antarctic, NO_2^- oxidizers are mixed into sunlit surface waters and experience light inhibition.

NO_3^--NO_2^- interconversion represents a previously unrecognized influence on NO_3^- N and O isotopic distributions in the Southern Ocean, and its consequences for our understanding of upper ocean NO_3^- isotope dynamics are not yet clear. If the isotopic signal of interconversion is preserved in the Antarctic mixed layer through the winter or develops early in the summer, then the $\delta^{15}N$ of phytoplankton (including diatoms) will be affected by it, with possible implications for the paleoceanographic record. In addition, intracellular, enzyme-level interconversion between NO_3^- and NO_2^- may help to explain previous evidence from tracer and natural abundance studies of NO_2^- oxidation in oxygen-deficient zones, a possibility that warrants further investigation.

Acknowledgments
The stable isotope data presented in this study will be merged into the P16S CCHDO product (http://cchdo.ucsd.edu/cruise/320620140320). This research was funded by the U.S. NSF through grant OPP-1401489 (D.M.S.), by the Princeton Environmental Institute's Undergraduate Research Fund for senior thesis research at Princeton University (P.C.K.), and by the Princeton University Department of Geosciences Fund for senior thesis research (P.C.K.). This is PMEL contribution 4518. R.Z. appreciates the support of the CSC Fellowship, and S.E.F. is grateful to the University of Cape Town URC fund. We thank S. Oleynik, W. Abouchami, and V. Luu for help with isotopic analyses and the captain and crew of the RVIB *Nathaniel B. Palmer* for a successful voyage.

References

Altabet, M. A., and R. Francois (2001), Nitrogen isotope biogeochemistry of the Antarctic Polar Frontal Zone at 170 W, *Deep Sea Res., Part II*, *48*(19), 4247–4273.

Begun, G. M., and W. H. Fletcher (1960), Partition function ratios for molecules containing nitrogen isotopes, *J. Chem. Phys.*, *33*(4), 1083–1085, doi:10.1063/1.1731338.

Beman, J. M., J. L. Shih, and B. N. Popp (2013), Nitrite oxidation in the upper water column and oxygen minimum zone of the eastern tropical North Pacific Ocean, *ISME J.*, *7*(11), 2192–2205, doi:10.1038/ismej.2013.96.

Brunner, B., et al. (2013), Nitrogen isotope effects induced by anammox bacteria, *Proc. Natl. Acad. Sci. U.S.A.*, *110*(47), 18,994–18,999, doi:10.1073/pnas.1310488110.

Buchwald, C., and K. L. Casciotti (2013), Isotopic ratios of nitrite as tracers of the sources and age of oceanic nitrite, *Nat. Geosci.*, *6*(4), 308–313, doi:10.1038/ngeo1745.

Buchwald, C., A. E. Santoro, R. H. R. Stanley, and K. L. Casciotti (2015), Nitrogen cycling in the secondary nitrite maximum of the eastern tropical North Pacific off Costa Rica, *Global Biogeochem. Cycles*, *29*, 2061–2081, doi:10.1002/2015GB005187.

Casciotti, K. L. (2009), Inverse kinetic isotope fractionation during bacterial nitrite oxidation, *Geochim. Cosmochim. Acta*, *73*(7), 2061–2076, doi:10.1016/j.gca.2008.12.022.

Casciotti, K. L., and M. R. McIlvin (2007), Isotopic analyses of nitrate and nitrite from reference mixtures and application to eastern tropical North Pacific waters, *Mar. Chem.*, *107*(2), 184–201, doi:10.1016/j.marchem.2007.06.021.

Casciotti, K. L., D. M. Sigman, M. G. Hastings, J. K. Böhlke, and A. Hilkert (2002), Measurement of the oxygen isotopic composition of nitrate in seawater and freshwater using the denitrifier method, *Anal. Chem.*, *74*(19), 4905–4912, doi:10.1021/ac020113w.

Casciotti, K. L., D. M. Sigman, and B. B. Ward (2003), Linking diversity and stable isotope fractionation in ammonia-oxidizing bacteria, *Geomicrobiol. J.*, *20*(4), 335–353, doi:10.1080/01490450390241035.

Casciotti, K. L., J. K. Böhlke, M. R. McIlvin, S. J. Mroczkowski, and J. E. Hannon (2007), Oxygen isotopes in nitrite: Analysis, calibration, and equilibration, *Anal. Chem.*, *79*(6), 2427–2436, doi:10.1021/ac061598h.

Casciotti, K. L., C. Buchwald, and M. McIlvin (2013), Implications of nitrate and nitrite isotopic measurements for the mechanisms of nitrogen cycling in the Peru oxygen deficient zone, *Deep Sea Res., Part I*, *80*, 78–93, doi:10.1016/j.dsr.2013.05.017.

Checkley, D. M., and C. A. Miller (1989), Nitrogen isotope fractionation by oceanic zooplankton, *Deep Sea Res., Part A*, *36*(10), 1449–1456, doi:10.1016/0198-0149(89)90050-2.

DiFiore, P. J., D. M. Sigman, K. L. Karsh, T. W. Trull, R. B. Dunbar, and R. S. Robinson (2010), Poleward decrease in the isotope effect of nitrate assimilation across the Southern Ocean, *Geophys. Res. Lett.*, *37*, L17601, doi:10.1029/2010GL044090.

Fawcett, S. E., M. W. Lomas, J. R. Casey, B. B. Ward, and D. M. Sigman (2011), Assimilation of upwelled nitrate by small eukaryotes in the Sargasso Sea, *Nat. Geosci.*, *4*(10), 717–722, doi:10.1038/ngeo1265.

Fawcett, S. E., M. W. Lomas, B. B. Ward, and D. M. Sigman (2014), The counterintuitive effect of summer-to-fall mixed layer deepening on eukaryotic new production in the Sargasso Sea, *Global Biogeochem. Cycles*, *28*, 86–102, doi:10.1002/2013GB004579.

Fawcett, S. E., B. B. Ward, M. W. Lomas, and D. M. Sigman (2015), Vertical decoupling of nitrate assimilation and nitrification in the Sargasso Sea, *Deep Sea Res., Part I*, *103*, 64–72, doi:10.1016/j.dsr.2015.05.004.

Friedman, S. H., W. Massefski, and T. C. Hollocher (1986), Catalysis of intermolecular oxygen atom transfer by nitrite dehydrogenase of *Nitrobacter agilis*, *J. Biol. Chem.*, *261*(23), 10,538–10,543.

Füssel, J., P. Lam, G. Lavik, M. M. Jensen, M. Holtappels, M. Günter, and M. M. Kuypers (2012), Nitrite oxidation in the Namibian oxygen minimum zone, *ISME J.*, *6*(6), 1200–1209, doi:10.1038/ismej.2011.178.

Gaye, B., B. Nagel, K. Dähnke, T. Rixen, and K. C. Emeis (2013), Evidence of parallel denitrification and nitrite oxidation in the ODZ of the Arabian Sea from paired stable isotopes of nitrate and nitrite, *Global Biogeochem. Cycles*, *27*, 1059–1071, doi:10.1002/2011GB004115.

Gordon, L. I., L. A. Codispoti, J. C. Jennings, F. J. Millero, J. M. Morrison, and C. Sweeney (2000), Seasonal evolution of hydrographic properties in the Ross Sea, Antarctica, 1996–1997, *Deep Sea Res., Part II*, *47*(15), 3095–3117, doi:10.1016/S0967-0645(00)00060-6.

Granger, J., and D. M. Sigman (2009), Removal of nitrite with sulfamic acid for nitrate N and O isotope analysis with the denitrifier method, *Rapid Commun. Mass Spectrom.*, *23*(23), 3753–3762, doi:10.1002/rcm.4307.

Granger, J., D. M. Sigman, J. A. Needoba, and P. J. Harrison (2004), Coupled nitrogen and oxygen isotope fractionation of nitrate during assimilation by cultures of marine phytoplankton, *Limnol. Oceanogr.*, *49*, 1763–1773, doi:10.4319/lo.2004.49.5.1763.

Granger, J., D. M. Sigman, M. F. Lehmann, and P. D. Tortell (2008), Nitrogen and oxygen isotope fractionation during dissimilatory nitrate reduction by denitrifying bacteria, *Limnol. Oceanogr.*, *53*(6), 2533, doi:10.4319/lo.2008.53.6.2533.

Granger, J., D. M. Sigman, M. M. Rohde, M. T. Maldonado, and P. D. Tortell (2010), N and O isotope effects during nitrate assimilation by unicellular prokaryotic and eukaryotic plankton cultures, *Geochim. Cosmochim. Acta*, *74*(3), 1030–1040, doi:10.1016/j.gca.2009.10.044.

Guerrero, M. A., and R. D. Jones (1996), Photoinhibition of marine nitrifying bacteria. II. Dark recovery after monochromatic or polychromatic irradiation, *Mar. Ecol. Prog. Ser.*, *141*(1), 193–198.

Hoch, M. P., M. L. Fogel, and D. L. Kirchman (1992), Isotope fractionation associated with ammonium uptake by a marine bacterium, *Limnol. Oceanogr.*, *37*(7), 1447–1459.

Karsh, K. L., J. Granger, K. Kritee, and D. M. Sigman (2012), Eukaryotic assimilatory nitrate reductase fractionates N and O isotopes with a ratio near unity, *Environ. Sci. Technol.*, *46*(11), 5727–5735, doi:10.1021/es204593q.

Karsh, K. L., T. W. Trull, D. M. Sigman, P. A. Thompson, and J. Granger (2014), The contributions of nitrate uptake and efflux to isotope fractionation during algal nitrate assimilation, *Geochim. Cosmochim. Acta*, *132*, 391–412, doi:10.1016/j.gca.2013.09.030.

Knox, F., and M. B. McElroy (1984), Changes in atmospheric CO_2: Influence of the marine biota at high latitude, *J. Geophys. Res.*, *89*(D3), 4629–4637, doi:10.1029/JD089iD03p0462.

Kritee, K., D. M. Sigman, J. Granger, B. B. Ward, A. Jayakumar, and C. Deutsch (2012), Reduced isotope fractionation by denitrification under conditions relevant to the ocean, *Geochim. Cosmochim. Acta*, *92*, 243–259, doi:10.1016/j.gca.2012.05.020.

Lehmann, M. F., S. M. Bernasconi, A. Barbieri, and J. A. McKenzie (2002), Preservation of organic matter and alteration of its carbon and nitrogen isotope composition during simulated and in situ early sedimentary diagenesis, *Geochim. Cosmochim. Acta*, *66*(20), 3573–3584, doi:10.1016/S0016-7037(02)00968-7.

Lipschultz, F., S. C. Wofsy, B. B. Ward, L. A. Codispoti, G. Friedrich, and J. W. Elkins (1990), Bacterial transformations of inorganic nitrogen in the oxygen-deficient waters of the eastern tropical South Pacific Ocean, *Deep Sea Res., Part A*, *37*(10), 1513–1541, doi:10.1016/0198-0149(90)90060-9.

Liu, K. K., S. J. Kao, K. P. Chiang, G. C. Gong, J. Chang, J. S. Cheng, and C. Y. Lan (2013), Concentration dependent nitrogen isotope fractionation during ammonium uptake by phytoplankton under an algal bloom condition in the Danshuei estuary, northern Taiwan, *Mar. Chem.*, *157*, 242–252, doi:10.1016/j.marchem.2013.10.005.

Lourey, M. J., Trull, T. W., and Sigman, D. M. (2003), Sensitivity of the $\delta^{15}N$ of surface suspended and deep sinking particulate organic nitrogen to Southern Ocean seasonal nitrate depletion, *Global Biogeochem. Cycles*, *17*(3), 1081, doi:10.1029/2002GB001973.

Mariotti, A., J. C. Germon, P. Hubert, P. Kaiser, R. Letolle, A. Tardieux, and P. Tardieux (1981), Experimental determination of nitrogen kinetic isotope fractionation: Some principles; illustration for the denitrification and nitrification processes, *Plant Soil*, *62*(3), 413–430, doi:10.1007/BF02374138.

Martin, J. H. (1990), Glacial-interglacial CO_2 change, *Paleoceanography*, *5*(1), 1–13, doi:10.1029/PA005i001p00001.

Martin, T. S., and K. L. Casciotti (2016), Nitrogen and oxygen isotopic fractionation during microbial nitrite reduction, *Limnol. Oceanogr.*, doi:10.1002/lno.10278.

Needoba, J. A., D. M. Sigman, and P. J. Harrison (2004), The mechanism of isotope fractionation during algal nitrate assimilation as illuminated by the $^{15}N/^{14}N$ of intracellular nitrate, *J. Phycol.*, *40*(3), 517–522, doi:10.1111/j.1529-8817.2004.03172.x.

Orsi, A. H., T. Whitworth, and W. D. Nowlin (1995), On the meridional extent and fronts of the Antarctic Circumpolar Current, *Deep Sea Res., Part I*, *42*(5), 641–673, doi:10.1016/0967-0637(95)00021-W.

Peloquin, J. A., and W. O. Smith (2007), Phytoplankton blooms in the Ross Sea, Antarctica: Interannual variability in magnitude, temporal patterns, and composition, *J. Geophys. Res.*, *112*, C08013, doi:10.1029/2006JC003816.

Peng, X., C. Fuchsman, A. Jayakumar, S. Oleynik, W. Martens-Habbena, A. Devol, and B. B. Ward (2015), Ammonia and nitrite oxidation in the eastern tropical North Pacific, *Global Biogeochem. Cycles*, *29*, 2034–2049, doi:10.1002/2015GB005278.

Pennock, J. R., D. J. Velinsky, J. M. Ludlam, J. H. Sharp, and M. L. Fogel (1996), Isotopic fractionation of ammonium and nitrate during uptake by *Skeletonema costatum*: Implications for $\delta^{15}N$ dynamics under bloom conditions, *Limnol. Oceanogr.*, *41*(3), 451–459, doi:10.4319/lo.1996.41.3.0451.

Pester, M., et al. (2014), NxrB encoding the beta subunit of nitrite oxidoreductase as functional and phylogenetic marker for nitrite-oxidizing *Nitrospira*, *Environ. Microbiol.*, *16*(10), 3055–3071, doi:10.1111/1462-2920.12300.

Rafter, P. A., P. J. DiFiore, and D. M. Sigman (2013), Coupled nitrate nitrogen and oxygen isotopes and organic matter remineralization in the Southern and Pacific Oceans, *J. Geophys. Res. Oceans*, *118*, 4781–4794, doi:10.1002/jgrc.20316.

Reuer, M. K., B. A. Barnett, M. L. Bender, P. G. Falkowski, and M. B. Hendricks (2007), New estimates of Southern Ocean biological production rates from O_2/Ar ratios and the triple isotope composition of O_2, *Deep Sea Res., Part I*, *54*(6), 951–974, doi:10.1016/j.dsr.2007.02.007.

Sarmiento, J. L., and J. R. Toggweiler (1984), A new model for the role of the oceans in determining atmospheric PCO_2, *Nature*, *308*(5960), 621–624, doi:10.1038/308621a0.

Sarmiento, J. L., N. Gruber, M. A. Brzezinski, and J. P. Dunne (2004), High-latitude controls of thermocline nutrients and low latitude biological productivity, *Nature*, *427*(6969), 56–60, doi:10.1038/nature02127.

Siegenthaler, U., and T. Wenk (1984), Rapid atmospheric CO_2, *Nature*, *308*, 12, doi:10.1038/308624a0.
Sigman, D. M., and E. A. Boyle (2000), Glacial/interglacial variations in atmospheric carbon dioxide, *Nature*, *407*(6806), 859–869, doi:10.1038/35038000.
Sigman, D. M., M. A. Altabet, D. C. McCorkle, R. Francois, and G. Fischer (1999), The $\delta^{15}N$ of nitrate in the Southern Ocean: Consumption of nitrate in surface waters, *Global Biogeochem. Cycles*, *13*(4), 1149–1166, doi:10.1029/1999GB900038.
Sigman, D. M., K. L. Casciotti, M. Andreani, C. Barford, M. Galanter, and J. K. Böhlke (2001), A bacterial method for the nitrogen isotopic analysis of nitrate in seawater and freshwater, *Anal. Chem.*, *73*(17), 4145–4153, doi:10.1021/ac010088e.
Sigman, D. M., J. Granger, P. J. DiFiore, M. M. Lehmann, R. Ho, G. Cane, and A. van Geen (2005), Coupled nitrogen and oxygen isotope measurements of nitrate along the eastern North Pacific margin, *Global Biogeochem. Cycles*, *19*, GB4022, doi:10.1029/2005GB002458.
Sigman, D. M., M. P. Hain, and G. H. Haug (2010), The polar ocean and glacial cycles in atmospheric CO_2 concentration, *Nature*, *466*(7302), 47–55, doi:10.1038/nature09149.
Smart, S. M., S. E. Fawcett, S. J. Thomalla, M. A. Weigand, C. J. Reason, and D. M. Sigman (2015), Isotopic evidence for nitrification in the Antarctic winter mixed layer, *Global Biogeochem. Cycles*, *29*, 427–445, doi:10.1002/2014GB005013.
Smith, J. M., F. P. Chavez, and C. A. Francis (2014), Ammonium uptake by phytoplankton regulates nitrification in the sunlit upper ocean, *PLoS One*, *9*, e108173.
Spindel, W. (1954), The calculation of equilibrium constants for several exchange reactions of nitrogen-15 between oxy compounds of nitrogen, *J. Chem. Phys.*, *22*(7), 1271–1272, doi:10.1063/1.1740370.
Sunda, W. G., and S. A. Huntsman (1997), Interrelated influence of iron, light and cell size on marine phytoplankton growth, *Nature*, *390*(6658), 389–392, doi:10.1038/37093.
Sundermeyer-Klinger, H., W. Meyer, B. Warninghoff, and E. Bock (1984), Membrane-bound nitrite oxidoreductase of *Nitrobacter*: Evidence for a nitrate reductase system, *Arch. Microbiol.*, *140*(2–3), 153–158, doi:10.1007/BF00454918.
Vanzella, A., M. A. Guerrero, and R. D. Jones (1989), Effect of CO and light on ammonium and nitrite oxidation by chemolithotrophic bacteria, *Mar. Ecol. Prog. Ser.*, *57*(1), 69–76.
Wada, E., and A. Hattori (1978), Nitrogen isotope effects in the assimilation of inorganic nitrogenous compounds by marine diatoms, *Geomicrobiol. J.*, *1*(1), 85–101, doi:10.1080/01490457809377725.
Walters, W. W., and G. Michalski (2015), Theoretical calculation of nitrogen isotope equilibrium exchange fractionation factors for various NO_y molecules, *Geochim. Cosmochim. Acta*, *164*, 284–297, doi:10.1016/j.gca.2015.05.029.
Ward, B. B. (1985), Light and substrate concentration relationships with marine ammonium assimilation and oxidation rates, *Mar. Chem.*, *16*, 301–316.
Ward, B. B. (2005), Temporal variability in nitrification rates and related biogeochemical factors in Monterey Bay, California, USA, *Mar. Ecol. Prog. Ser.*, *292*(97), 109.
Waser, N. A. D., P. J. Harrison, B. Nielsen, S. E. Calvert, and D. H. Turpin (1998), Nitrogen isotope fractionation during the uptake and assimilation of nitrate, nitrite, ammonium, and urea by a marine diatom, *Limnol. Oceanogr.*, *43*(2), 215–224, doi:10.4319/lo.1998.43.2.0215.
Weigand, M. A., J. Foriel, B. Barnett, S. Oleynik, and D. M. Sigman (2016), Updates to instrumentation and protocols for isotopic analysis of nitrate by the denitrifier method, *Rapid Commun. Mass Spectrom.*, *30*(12), 1365–1383, doi:10.1002/rcm.7570.
Wunderlich, A., R. U. Meckenstock, and F. Einsiedl (2013), A mixture of nitrite-oxidizing and denitrifying microorganisms affects the $\delta^{18}O$ of dissolved nitrate during anaerobic microbial denitrification depending on the $\delta^{18}O$ of ambient water, *Geochim. Cosmochim. Acta*, *119*, 31–45.